Cell, Vol. 89, 127–138, April 4, 1997, Copyright ©1997 by Cell Press

Redefining the Genetic Hierarchies Controlling Skeletal Myogenesis: *Pax-3* and *Myf-5* Act Upstream of *MyoD*

Shahragim Tajbakhsh,* Didier Rocancourt,*
Giulio Cossu,† and Margaret Buckingham*
*Department of Molecular Biology
Centre National de la Recherche Scientifique
Unité de Recherche Associé 1947
Pasteur Institute
75724 Paris, Cedex 15
France
†Department of Histology and Medical Embryology
University of Rome, La Sapienza
00161 Rome
Italy

Summary

We analyzed *Pax-3* (*splotch*), *Myf-5* (targeted with *nlacZ*), and *splotch*/*Myf-5* homozygous mutant mice to investigate the roles that these genes play in programming skeletal myogenesis. In *splotch* and *Myf-5* homozygous embryos, myogenic progenitor cell perturbations and early muscle defects are distinct. Remarkably, *splotch*/*Myf-5* double homozygotes have a dramatic phenotype not seen in the individual mutants: body muscles are absent. *MyoD* does not rescue this double mutant phenotype since activation of this gene proves to be dependent on either Pax-3 or Myf-5. Therefore, *Pax-3* and *Myf-5* define two distinct myogenic pathways, and *MyoD* acts genetically downstream of these genes for myogenesis in the body. This genetic hierarchy does not appear to operate for head muscle formation.

Introduction

During vertebrate embryogenesis, paraxial mesoderm flanking the neural tube becomes segmented into epithelial spheres called somites, which subsequently become compartmentalized into a dorsal epithelial dermomyotome (muscle and dermis) and a ventral mesenchymal sclerotome (vertebral column and ribs). Myogenic progenitor cells in the dermomyotome give rise to all of the skeletal muscles of the body (trunk and limb) and some head muscles, while the remaining head muscles arise from more anterior nonsomitic paraxial and prechordal head mesoderm (reviewed by Wachtler and Christ, 1992; Christ and Ordahl, 1995).

Manipulations in avian embryos have shown that cells in the epithelial somite are multipotent and will adopt a particular somitic fate according to their position in relation to surrounding structures (Christ and Ordahl, 1995). This conclusion is also supported by explant experiments with early somites and presomitic mesoderm (reviewed by Cossu et al., 1996b). Activation of myogenesis in medially located muscle progenitor cells in the dermomyotome depends on axial structures (neural tube and notochord) leading to myotome formation in the central aspect of the somite. Cells in this (dorsal) domain of the myotome subsequently form the epaxial (deep back) muscles. In contrast, myogenic activation in the lateral dermomyotome depends on the presence of dorsal ectoderm (Kenny-Mobbs and Thorogood, 1987; Fan and Tessier-Lavigne, 1994; Cossu et al., 1996a) and is repressed by lateral mesoderm (Cossu et al., 1996a; Pourquié et al., 1996). Muscle progenitors in the lateral dermomyotome contribute to the ventral aspect of the myotome, which will form the hypaxial (e.g., abdominal and body wall) muscles of the body (Christ and Ordahl, 1995). At the limb levels, cells destined to form skeletal muscle migrate from the lateral dermomyotome into the limb field. At this stage they do not express any myogenic regulatory factors (MRFs) or other skeletal muscle markers (Sassoon et al., 1989; Tajbakhsh and Buckingham, 1994).

The basic–helix-loop-helix (bHLH) MRFs Myf-5, MyoD, myogenin, and MRF4 act as transcriptional activators of skeletal muscle genes, and their forced expression in many nonmuscle cell types induces the skeletal muscle differentiation program (reviewed by Weintraub et al., 1991). Gene knockout experiments have shown that although *Myf-5* null (Braun et al., 1992) or *MyoD* null (Rudnicki et al., 1992) mice make muscle, *Myf-5*/*MyoD* double mutants are devoid of muscle fibers and myoblasts (Rudnicki et al., 1993). *myogenin* null mice have virtually no muscle fibers but myoblasts appear normal (Hasty et al., 1993; Nabeshima et al., 1993), suggesting that this gene is necessary for terminal differentiation, whereas *MRF4* null mice have no prominent muscle defects (reviewed by Olson et al., 1996). It is therefore believed that *Myf-5* and *MyoD* can compensate for each other and together act in a genetic pathway upstream of *myogenin* and *MRF4* to program all skeletal myogenesis. In the mouse, Myf-5 is the first MRF to be expressed in the somite (Ott et al., 1991; Buckingham, 1992), prior to myotome formation and about 2 days before *MyoD* activation. During this developmental period, muscle progenitor cells that have activated *Myf-5* remain multipotent and can change their fate in the absence of Myf-5 protein. This occurs as a result of an aberrant migration and mislocalization of these cells in *Myf-5* null embryos (Tajbakhsh et al., 1996b). In explant experiments, *Myf-5* is the first MRF gene to be induced by axial structures, which correlates with its early expression in the dorsomedial part of the somite adjacent to the neural tube, whereas *MyoD* appears to be induced more rapidly in response to dorsal ectoderm. Subsequently, *Myf-5* and *MyoD* are coexpressed in the majority of cells with myogenic potential both in vitro and in the embryo (Cossu et al., 1996a; Tajbakhsh et al., 1996a).

Pax-3, a mammalian homolog of the Drosophila *paired* gene, encodes a transcription factor and belongs to a family of developmentally regulated genes (Strachan and Read, 1994). In the mouse, *Pax-3* and the closely related paired box gene *Pax-7* are expressed in mesodermal and neuroectodermal derivatives. Mice heterozygous for mutations in *Pax-3* (*splotch* [*Sp*]) are characterized by pigmentation defects due to perturbations in neural crest migration, whereas homozygous embryos have a number of neural defects, including spina bifida

and exencephaly (reviewed by Tremblay and Gruss, 1994). Most homozygous mutant *Sp* alleles are lethal prior to embryonic day 15 (E15). *Pax-3* is expressed in the unsegmented paraxial mesoderm (UPM) and epithelial somite, becoming confined first to the dermomyotome and later to its lateral half. Cells that migrate from the lateral part of the somite to the limb express *Pax-3* (Williams and Ordahl, 1994; Daston et al., 1996). Indeed, *Sp* mice lack limb muscles, demonstrating that *Pax-3* is necessary for the migration of this muscle precursor cell population (Bober et al., 1994; Goulding et al., 1994; Marcelle et al., 1995). This phenotype is similar to that of mice carrying a null mutation in the *met* receptor gene (Bladt et al., 1995; Maina et al., 1996), and recent results suggest that Pax-3 may directly activate the *met* gene (Epstein et al., 1996; Yang et al., 1996). The latter is also expressed in the dermomyotome, and muscle precursor cells expressing *met* may migrate in response to its ligand, scatter factor, which is present in the proximal limb (Bladt et al., 1995).

Since *Pax-3* and *Myf-5* are expressed in muscle progenitor cells, we analyzed loss-of-function mutations in single and double mutant mice to investigate the respective roles that the *Pax-3* and *Myf-5* genes play in programming myogenesis. While the individual mutations display perturbations in some distinct skeletal muscles, strikingly, in *Sp/Myf-5* double homozygous mutant embryos, skeletal muscles in the body are ablated. In the absence of Pax-3 and Myf-5, *MyoD* is not activated in the body and therefore cannot rescue skeletal myogenesis, suggesting that it acts genetically downstream from *Pax-3* and *Myf-5*. Moreover, neither *Pax-3* nor *Pax-7* is detectable in skeletal muscle progenitors of the head, suggesting that myogenic regulatory circuits in the head and body are distinct.

Results

Migrating Muscle Populations Are Absent in *Sp* Mice

We crossed *Sp* with *Myf-5/nlacZ* (*Myf-5*$^{a2+/-}$) heterozygous mice to facilitate the analysis of skeletal muscle perturbations and patterning in the absence of *Pax-3*. As expected, limb muscles were missing in *Sp/Myf-5*$^{a2+/-}$ embryos (Figure 1C). However, other skeletal muscle perturbations were also detected. The latissimus dorsi muscle, originating just posterior to the forelimb and later spanning dorsoventrally in the interlimb region, is absent in *Sp* homozygous embryos (Figures 1A, 1C, 2A, and 2B). Muscles of the shoulder, ventral body, and diaphragm (Figure 2F) also were missing. In addition, from about embryonic day 10 (E10), muscle progenitor cells originating from the occipital somites undergo a long-range migration underneath the arches to constitute the hypoglossal muscles of the throat and some tongue musculature. These cells, which activate *Pax-3* initially and subsequently express Myf-5, MyoD, and myogenin, were absent in *Sp* homozygous embryos at E10.5 (Figures 4C, 4H, and 4L and data not shown).

These findings suggest that migrating muscle progenitor cells in the lateral-half somite, which express *Pax-3* prior to activation of *Myf-5* or *MyoD* (see below), are largely absent in *Sp* homozygous embryos. It is noteworthy that some deep back muscles derived from the medial-half somite were also noticeably absent in *Sp/Myf-5*$^{a2+/-}$ embryos by E12.5 (Figure 1C).

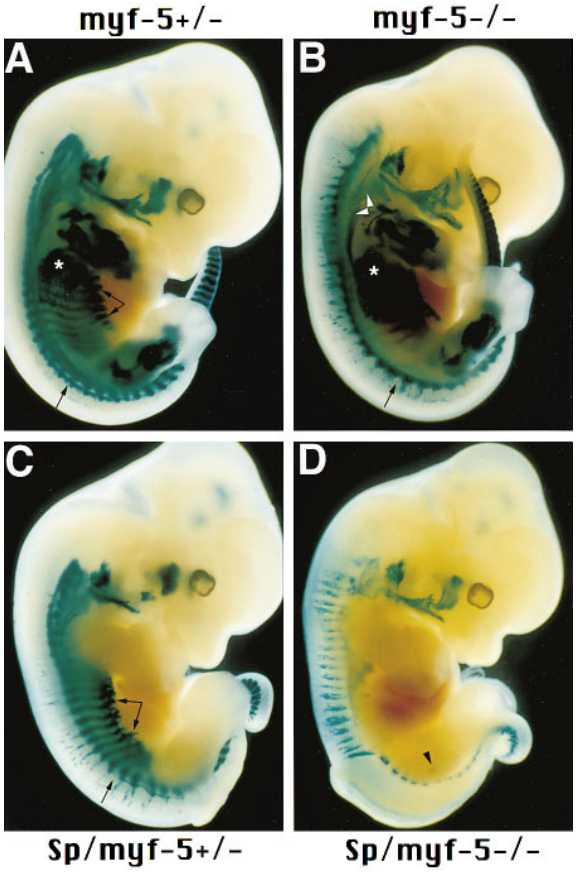

Figure 1. Skeletal Muscle Perturbations Are Distinct in *Sp* and *Myf-5*$^{a2-/-}$ Homozygous Mutant Embryos

E12.5 embryos were analyzed by X-Gal staining in toto.

(A) *Myf-5*$^{a2+/-}$ embryo. The forming latissimus dorsi muscle (asterisk), deep back (arrow), and intercostal (double arrows) muscles are indicated.

(B) *Myf-5*$^{a2-/-}$ embryo showing deep back (arrow) and shoulder muscle perturbations. Notably, a shoulder muscle group opposite and anterior to the forelimb (arrowheads), which activates *MyoD* relatively early, is less perturbed.

(C) *Sp/Myf-5*$^{a2+/-}$ embryo with deep back muscle perturbations (arrow) distinct from those in the *Myf-5*$^{a2-/-}$ embryo. Intercostal muscles appear properly segmented but have a shortening and disorganization of their most ventral extent (double arrows).

(D) *Sp/Myf-5*$^{a2-/-}$ embryo showing β-gal^{+} cells in a segmented organization extending dorsally. A few β-gal^{+} cells are also seen in the hindlimb (arrowhead). Lack of limb muscles and spina bifida in the caudal neural tube (failure to close) distinguish the *Sp* mutants.

Skeletal Muscle Perturbations Are Distinct in *Sp* Homozygous and *Myf-5* Null Mice

Myf-5 null mice carrying the bacterial *nlacZ* reporter gene under the control of *Myf-5* regulatory sequences (Tajbakhsh et al., 1996b) reproduce the delay in myotome formation, truncated rib phenotype, and perinatal death described for another allele at this locus (Braun et al., 1992). We have shown that *nlacZ* faithfully recapitulates *Myf-5* expression in these mice (Tajbakhsh and

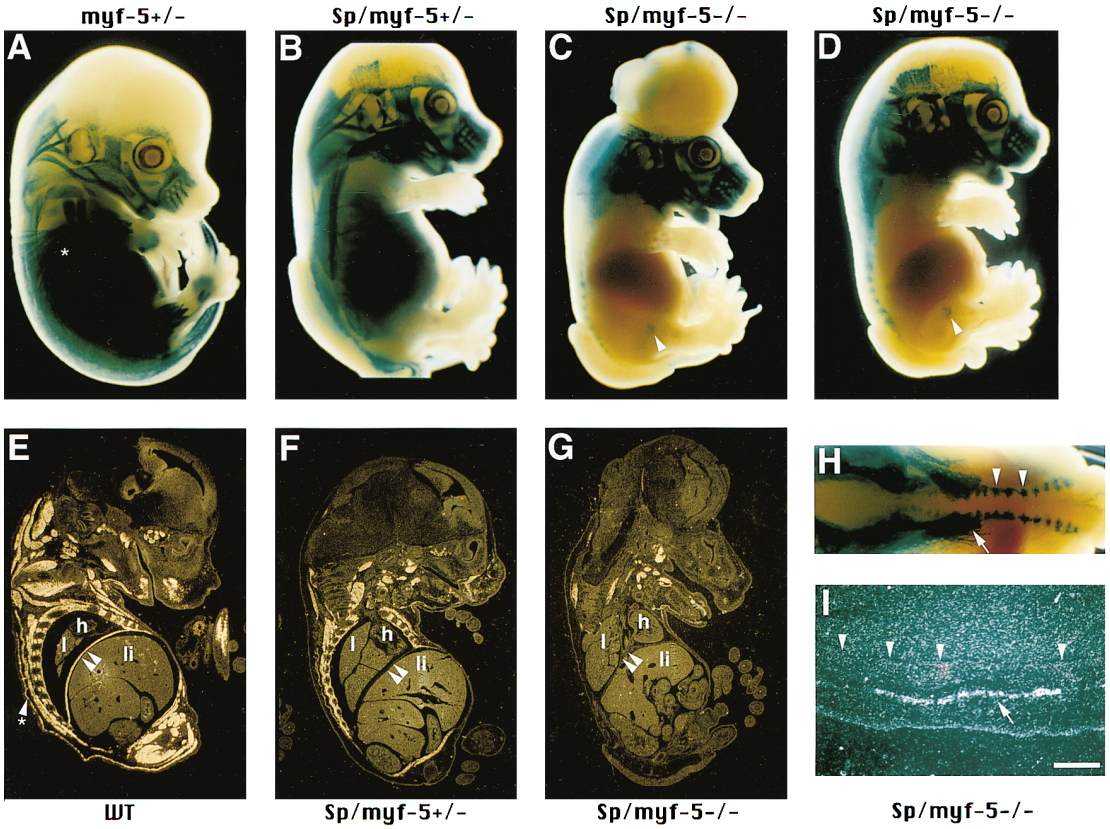

Figure 2. Skeletal Muscles Are Ablated in the Body of *Sp/Myf-5*$^{a2-/-}$ Double Homozygous Embryos

E14.5 *Myf-5*$^{a2+/-}$ (A), *Sp/Myf-5*$^{a2+/-}$ (B), and *Sp/Myf-5*$^{a2-/-}$ (C with exencephaly, D, and H) embryos were analyzed by X-Gal staining in toto. The *Myf-5*$^{a2+/-}$ embryo was stained more briefly with X-Gal to distinguish muscle groups more clearly. The prominent latissimus dorsi muscle (A and E, asterisk) is missing in *Sp* embyros (B, C, D, F, and G). Some β-gal^{+} cells are reproducibly detected in the hindlimb of *Sp* mutants (C and D, arrowheads). (E, F, G, and I) In situ hybridizations with an antisense myogenin riboprobe on saggital sections of wild-type (E), *Sp/Myf-5*$^{a2+/-}$ (F), and *Sp/Myf-5*$^{a2-/-}$ (G and I) E14.5 embryos, visualized by dark-field microscopy. Note the absence of diaphragm muscle (double arrowheads) and some neck and shoulder muscles in embryos mutant for *Pax-3* (F and G). In toto X-Gal stained (H) and saggital section reacted with a myogenin riboprobe (I) of a *Sp/Myf-5*$^{a2-/-}$ embryo reveals that the metameric β-gal expression, appearing as pink in dark field (underneath the neck muscles on whole mount), is myogenin negative (arrowheads) while the neck muscles are myogenin positive (arrow). l, lung; li, liver, h, heart. Scale bar, 150 μm (E–G) and 40 μm (I).

Buckingham, 1995; Tajbakhsh et al., 1996a). The ability to readily monitor β-galactosidase–positive (β-gal^{+}) cells and muscles by whole-mount coloration permitted us to detect early skeletal muscle perturbations that were not reported previously (Braun et al., 1992; Braun et al., 1994).

The skeletal muscle defects observed in *Sp* homozygotes were qualitatively distinct from those in *Myf-5* null mice (Figures 1B and 1C). Prior to *MyoD* activation, the early myotome is absent in *Myf-5* null mice, and β-gal^{+} muscle progenitor cells are disorganized (Tajbakhsh et al., 1996b; Figure 4B). Subsequently, at E12.5, a stage when MyoD is normally present (Sassoon et al., 1989), perturbations extending along the anterior–posterior axis were evident, particularly in the deep back and dorsal and ventral interlimb muscles (Figure 1B). Some of the ventral disorganization in the thoracic region may be due to the truncated rib phenotype. The skeletal muscle deficiencies observed at early stages in *Myf-5*$^{a2-/-}$ embryos were less prominent after E14.5 (data not shown). Both *Pax-3* and *Myf-5* are therefore important in the establishment of skeletal muscles in the body at early developmental stages.

Body Muscles Are Ablated in *Sp/Myf-5* Double Homozygous Mice

To determine which aspects of skeletal muscle development are controlled by *Pax-3* and *Myf-5*, we interbred double heterozygous *Sp*/+/*Myf-5*$^{a2+/-}$ mice to obtain double homozygous mutants. As expected, *Sp* and *Myf-5*$^{a2-/-}$ homozygous embryos were not viable. Double heterozygous mice were viable and fertile and were used as breeding stocks. No obvious skeletal muscle abnormalities were seen in these animals.

Strikingly, analysis of double homozygous mutant embryos revealed that *nlacZ* expression in the body was almost entirely eliminated, whereas head muscles were apparently normal (Figures 1D, 2C, and 2D). To determine whether this observation does not reflect merely a down- regulation of the *Myf-5* promoter, we analyzed saggital sections for the presence of transcripts of the muscle differentiation marker *myogenin*. In situ hybridization revealed that myogenin expression was absent in the body of these animals but was present in the head (Figure 2G). Examination of fetuses in whole mount and sections showed that the double mutants have a reduced size in the back and body wall regions compared

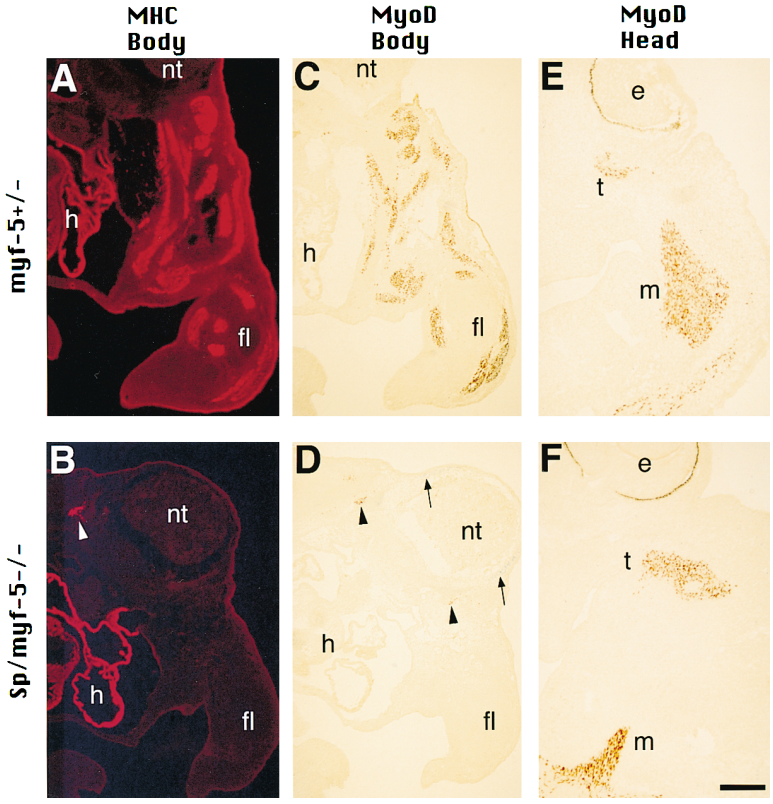

Figure 3. MyoD and MHC Expression Are Ablated in the Body of *Sp/Myf-5*$^{a2-/-}$ Double Homozygous Embryos

Serial transverse cryostat sections from X-Gal–stained E12.5 *Myf-5*$^{a2+/-}$ (A, C, and E) and *Sp/Myf-5*$^{a2-/-}$ (B, D, and F) embryos were reacted either with a fluorescence- labeled anti-MHC (A and B) or a peroxidase-labeled anti-MyoD (C–F) antibody. A small group of cells adjacent to the neural tube is positive for both markers in the double mutant (B and D, arrowheads). Arrows (D) indicate aberrantly located β-gal$^+$ cells seen more proximally and dorsally. e, eye; fl, forelimb; h, cardiac muscle; m, masseter; nt, neural tube; t, temporalis. Scale bar, 30 μm (A–D) and 15 μm (E and F).

to *Sp* homozygous or wild-type littermates (Figures 2 and 3 and data not shown). Occasionally, traces of myogenin expression were observed in the body of double mutants (data not shown).

Although *Myf-5* expression was almost entirely ablated in the body of *Sp/Myf-5*$^{a2-/-}$ double homozygous embryos, some β-gal$^+$ regions were detected reproducibly in the body of these mutants (Figures 2C, 2D, and 2H; see also below). A few β-gal$^+$ cells appearing in a segmental organization were detected dorsally (Figure 2H), and a group of β-gal$^+$ cells was observed in the proximal region of the hindlimb (Figures 2C and 2D). In addition, some neck muscles that appear to extend from the head into the body of the embryo were observed in these double mutants (Figure 2H). To evaluate the nature of these β-gal$^+$ cells in the body, we examined saggital sections from E14.5 *Sp/Myf-5*$^{a2-/-}$ embryos that were stained for β-gal activity and then hybridized with an antisense *myogenin* probe (Figures 2H and 2I). Our analysis revealed that β-gal$^+$ cells in the hindlimb and dorsal body were negative for myogenin, with some of these cells appearing in cartilage (Figure 2I and data not shown). These observations suggest that they are mislocated muscle progenitor cells, as described in *Myf-5* null embryos at early stages (Tajbakhsh et al., 1996b). The neck muscles, however, transcribe the *myogenin* gene.

To analyze further this muscle phenotype, we used an anti–myosin heavy chain (MHC) antibody that recognizes the major striated muscle isoforms of this family. Whereas skeletal muscles in the trunk and limb as well as cardiac muscle were positive with this antibody in E12.5 *Myf-5*$^{a2+/-}$ embryos, *Sp/Myf-5*$^{a2-/-}$ double homozygous embryos lacked MHC expression in the trunk and limbs while labeling in the heart appeared normal (Figures 3A and 3B). MyoD protein expression also was ablated in these double mutants (see below).

Therefore, we conclude that skeletal muscles of the body are ablated in *Sp/Myf-5*$^{a2-/-}$ double homozygous embryos while head muscles are present. Given the latter finding, we examined the expression of *Pax-3* and *Pax-7* in muscle precursors and developing muscles of the body and head by whole-mount in situ hybridization (Figures 4K–4N and data not shown). Both genes were expressed in the somites, with *Pax-7* in the central dermomyotome (Figure 4M) and *Pax-3* more laterally (Figure 4K), and both were expressed in skeletal muscles at later stages (data not shown). However, neither *Pax-3* nor *Pax-7* transcripts were detectable in forming skeletal muscles or their precursors in the head (Figures 4K and 4M and data not shown). The expression pattern of *Pax-7* did not appear to be significantly altered in the body or head of *Sp* homozygous embryos (Figure 4N and data not shown). Furthermore, *Pax-7* is expressed later than *Pax-3*, and *Pax-7* null mice do not appear to have a muscle phenotype (Mansouri et al., 1996).

Distinct Muscle Progenitor Cell Perturbations in *Sp*, *Myf-5*, and *Sp/Myf-5* Homozygous Mutant Embryos

To understand the respective roles that *Pax-3* and *Myf-5* play in programming myogenesis, we examined

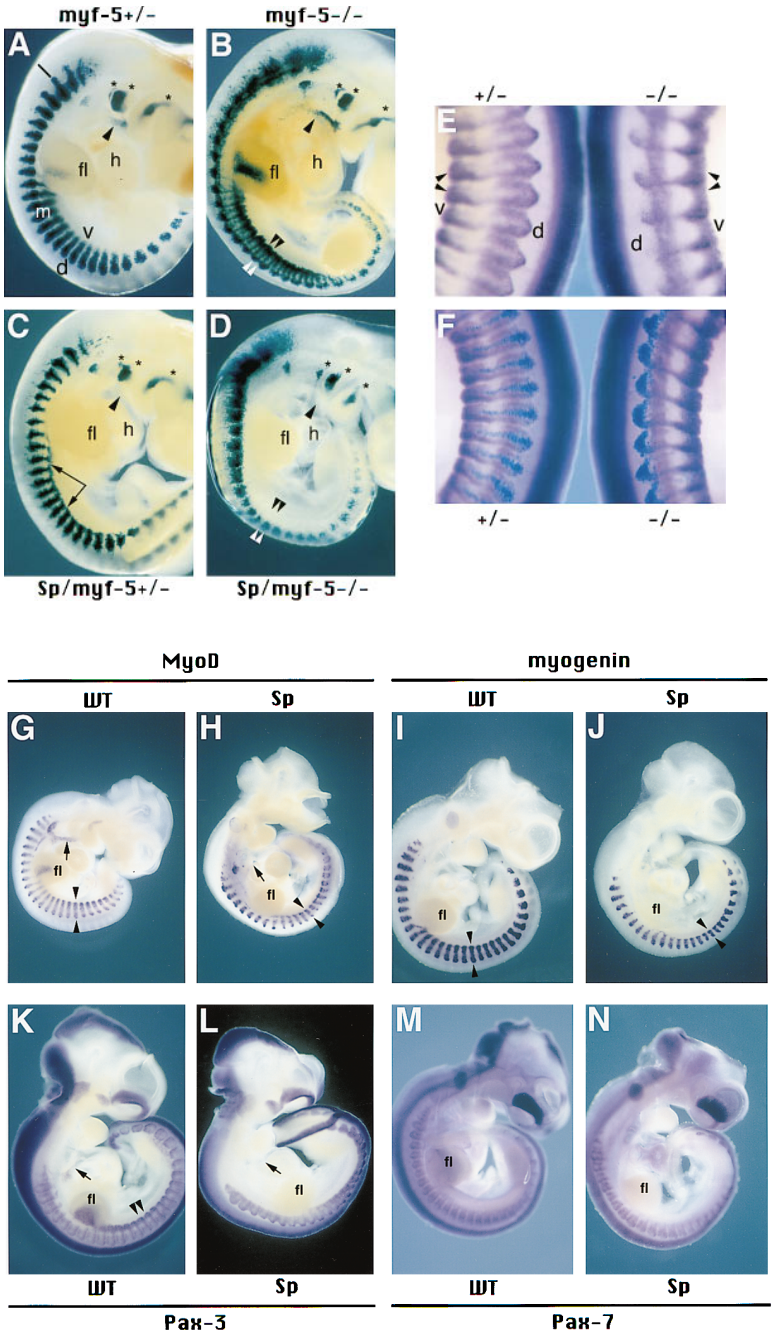

Figure 4. Perturbations in *Pax-3* and *MRF* Expression in Mutant Embryos

E10.5 mutant embryos were analyzed by X-Gal staining in toto (A–D).

(A) *Myf-5*$^{a2+/-}$ embryo showing β-gal^{+} cells in the forelimb (fl). The dorsal (d) and ventral (v) domains of the myotome (m) overlap. Muscle precursors in the hypoglossal chord are indicated (arrowhead), anterior to the heart (h). Bar indicates first cervical somite, anterior to which are the occipital somites.

(B) *Myf-5*$^{a2-/-}$ embryo showing muscle progenitor cell perturbations in all somites, particularly those in the interlimb region where epaxial and hypaxial progenitors accumulate (double arrowheads) along the dorsal (white) and ventral (black) edges of the somite.

(C) *Sp/Myf-5*$^{a2+/-}$ embryo showing an expanded pattern of β-gal^{+} cells ventrally in adjacent somites (double arrows; see also H and J).

(D) *Sp/Myf-5*$^{a2-/-}$ embryo showing β-gal^{+} cells in the ventral domain of interlimb somites are missing (black double arrowheads). In all embryos, muscle precursors of the arches (asterisks) are present.

(E and F) Whole-mount in situ hybridizations using an antisense *Pax-3* probe (purple) on E11.5 unstained (E) and briefly X-Gal–stained (F, blue) *Myf-5*$^{a2+/-}$ and *Myf-5*$^{a2-/-}$ embryos (interlimb region shown). Ventral (v) staining of Pax-3 corresponds to the epithelial somitic bud in the distal-most dermomyotome in the heterozygote (double arrowheads), while dorsal (d) staining in the cytoplasm of myotomal cells surrounds the β-gal^{+} nuclei. A continuous intense staining in the neural tube can also be observed with the *Pax-3* probe.

(G–N) Whole-mount in situ hybridizations on E10.5 wild-type (G, I, K, and M) and *Sp* homozygous (H, J, L, and N) embryos using antisense *MyoD* (G and H), myogenin (I and J), *Pax-3* (K and L), and *Pax-7* (M and N probes). The hypoglossal chord (arrow) and forelimb (fl) labeling is absent in *Sp* embryos (H and L), and the ventral and dorsal myotome are reduced (H and J, opposing arrowheads) as in (C). *Pax-3* expression in somites is more concentrated in the lateral domain (double arrowheads).

the patterning of muscle progenitor (β-gal^{+}) cells in *Sp/Myf-5*$^{a2+/-}$ *and Sp/Myf-5*$^{a2-/-}$ embryos at an earlier stage. In normal *Myf-5*$^{a2+/-}$ embryos, the myotome was well established by E10.5 (Figure 4A) and contained differentiated myocytes expressing skeletal muscle markers. At this stage, the dorsal (epaxial) and ventral (hypaxial) domains of the myotome overlap, rendering this division indistinguishable with available muscle markers. In addition, the forelimbs contain Pax-3^{+} and β-gal^{+} muscle precursor cells. In *Myf-5*$^{a2-/-}$ embryos, the myotome was absent and muscle progenitor cells were aberrantly blocked along the medial edge of all somites and along the lateral edge of interlimb (Figure 4B) and tail (data not shown) somites. In *Sp/Myf-5*$^{a2+/-}$ embryos, the myotome was present; however, a noticeable shortening and disorganization of the somitic bud (lateral-most dermomyotome) of interlimb somites as well as a subtle decrease in size of the medial somitic domain were seen (Figures 4C, 4H, 4J, and 4L; see also Figure 1C).

Notably, in *Sp/Myf-5*$^{a2-/-}$ double homozygous embryos, β-gal expression was absent in the ventrolateral aspect of interlimb somites at E10.5 (Figure 4D). In contrast, β-gal expression was observed in dorsomedial muscle progenitors, but they appeared disorganized

and slightly more dispersed than in *Myf-5*$^{a2-/-}$ embryos (compare Figures 4B and 4D). This labeling corresponded to the ectopic β-gal$^+$ cells observed dorsally at later stages (Figures 1D, 2H, and 3D). In all mutants examined, the arches, temporalis, and extraocular muscles of the head appeared normal (Figures 4A–4D and data not shown). Thus, *Myf-5* activation is independent of Pax-3 except in the ventrolateral domain in interlimb somites (see Discussion).

To determine whether *Pax-3* expression is dependent on *Myf-5*, we analyzed *Myf-5*$^{a2+/-}$ and *Myf-5*$^{a2-/-}$ embryos by whole-mount in situ hybridization with antisense *Pax-3* combined with X-Gal staining. In normal embryos, *Pax-3* expression is confined to the somitic bud of the dermomyotome by E10.5 (Figure 4K). A reactivation of *Pax-3* then occurs in the medial aspect of the myotome (Figures 4E and 4F and data not shown). As muscle progenitor cells leave the lateral dermomyotome to form the ventral myotome, *Pax-3* expression is down-regulated. The activation of *Pax-3* was unaffected in the *Myf-5* null mutants; however, qualitative differences in the expression pattern were observed in interlimb somites (Figures 4E and 4F). An expanded *Pax-3* expression pattern laterally corresponds to the aberrant myogenic progenitor cell accumulation along this edge of the dermomyotome. These β-gal$^+$ muscle progenitor cells continued to express *Myf-5* and *Pax-3* (Figures 4B, 4E, and 4F and data not shown). In contrast, those leaving the medial somite appeared more dorsally and were Pax-3 negative.

These findings demonstrate that, although qualitative and quantitative differences in muscle progenitor cell migrations and patterning were observed in *Sp* homozygous and *Myf-5* null mutants, *Pax-3* and *Myf-5* genes are activated independently of each other. Furthermore, *Pax-3* expression in the somite precedes that of *Myf-5*; it is *Myf-5*, however, that programs early myogenesis to form the myotome.

MyoD Is Activated in Body Muscles of *Sp* Homozygous but Not *Sp/Myf-5* Double Homozygous Embryos

It is believed that in *Myf-5* null mice, Myf-5–independent activation of *MyoD* rescues the myogenic program (Braun et al., 1994) and that either Myf-5 or MyoD is essential for skeletal muscle formation (Rudnicki et al., 1993). It was therefore important to determine whether *MyoD* is activated normally in *Sp* homozygous and *Sp/Myf-5*$^{a2-/-}$ double homozygous embryos. Figure 4H shows by whole-mount in situ hybridization that *MyoD* transcripts were detectable in all somites of *Sp* homozygous embryos at E10.5, the time when *MyoD* becomes activated in wild-type embryos (see below). This expression pattern, which is qualitatively similar to that of *myogenin* (Figures 4H and 4J), reflects the skeletal muscle perturbations observed in *Sp/Myf-5*$^{a2+/-}$ embryos at this stage (see Figure 4C).

We then examined MyoD expression in *Sp/Myf-5*$^{a2-/-}$ double homozygous embryos. Figures 3C and 3D show that MyoD protein was lacking in the trunk and limbs of these mutants but was present in head muscles (Figures 3E and 3F). *MyoD* transcripts were not detected in the body on saggital sections of E14.5 double mutant embryos (data not shown). Furthermore, these regions were negative for the early myoblast marker desmin (data not shown). It is noteworthy that in *Sp/Myf-5*$^{a2-/-}$ double homozygous embryos, a few MyoD$^+$ cells that were also MHC$^+$ were detected in the trunk adjacent to the neural tube at E12.5 (Figures 3B and 3D). It is not clear whether these cells originated from the epaxial or hypaxial domain of the somite. This expression is reminiscent of the residual myogenin-positive cells observed in the trunk at E14.5. In addition, neither anti-MyoD nor anti-MHC (Figure 3D) nor anti-desmin (data not shown) antibodies marked the ectopically located β-gal$^+$ cells that appeared dorsally, adjacent to the neural tube at this stage (see also Figure 1D). These findings confirm that the precursor muscle cell population is almost entirely absent in the body of these double homozygous embryos.

MyoD Activation Is Delayed in *Myf-5* Null Mice

Since back muscle perturbations were observed in *Myf-5* null mice 2 days after the expected activation of *MyoD* (Figure 1B), we examined the onset of *MyoD* expression in normal and *Myf-5* null mice, both at the transcriptional and at the translational level. Interlimb somites were analyzed to facilitate the simultaneous monitoring of medial and lateral myogenesis and to avoid potential confusion with more anterior shoulder muscles, which do not show the approximately 2-day delay in activation between *Myf-5* and *MyoD* (Figure 1B).

MyoD expression appeared relatively synchronously in the dorsal myotome of all somites at E10 (about 33 somites; Figure 4G), whereas earlier expression, at E9.75, (about 30 somites) occurred in the ventral myotome of interlimb somites, following a rostrocaudal gradient. Transcripts of *Myf-5* were also detected in this domain but at considerably lower levels than in the medial somite (data not shown). A comparative analysis of E10.75 wild-type, heterozygous, and homozygous embryos, stained briefly with X-Gal, revealed that *MyoD* transcripts were not detectable in the somites of *Myf-5* null embryos (Figures 5A and 5B) and were present at a reduced level compared to that in normal embryos at E11.5 (data not shown). Wild-type and *Myf-5*$^{a2+/-}$ embryos gave similar intensity staining with the *MyoD* probe (Figure 5A). The whole-mount staining reaction was stopped prior to saturation of the signal in order to distinguish differences more clearly. Experiments on non–X-Gal stained embryos gave similar results. These results were not dependent on the genetic backgound of the embryos, since a comparison of embryos obtained from a mixed genetic background (see Experimental Procedures) with those from outbred mice gave similar results.

To confirm these findings, we monitored MyoD protein accumulation. Sections through thoracic somites of *Myf-5*$^{a2+/-}$ and *Myf-5*$^{a2-/-}$ embryos at E11 showed that while most cells expressed both β-gal and MyoD in the myotome of the *Myf-5*$^{a2+/-}$ embryo (Figures 5C and 5D), considerably fewer cells expressing MyoD protein were detected in *Myf-5*$^{a2-/-}$ embryos (Figure 5F). MHC accumulation showed a similar delay in *Myf-5* null mutants (data not shown). Therefore, we conclude that there is

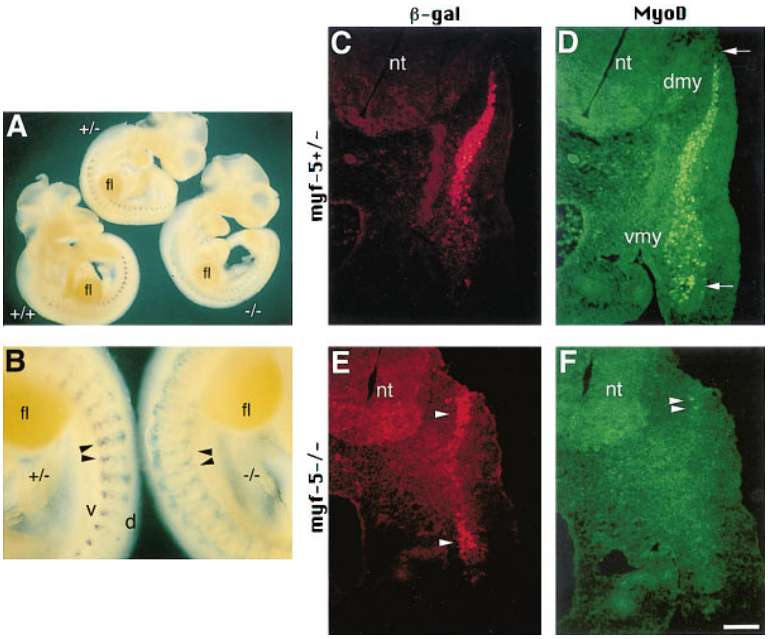

Figure 5. *MyoD* Activation Is Delayed in *Myf-5*$^{a2-/-}$ Embryos

(A) Wild-type, *Myf-5*$^{a2+/-}$, and *Myf-5*$^{a2-/-}$ embryos from E10.75 (39 somite) outbred mice were stained briefly with X-Gal and then whole-mount in situ hybridized with an antisense *MyoD* probe. Both the wild-type and *Myf-5*$^{a2+/-}$ embryos reveal *MyoD* transcript accumulation in the ventral domain of interlimb somites and dorsally in more anterior somites.

(B) Enlargement of the interlimb region of the heterozygous and homozygous mutant embryos in (A). The X-Gal labeling (blue, dorsally, d) is distinct from the MyoD signal (purple, ventrally, v; double arrowheads) and distinguishes the heterozygous from the homozygous embryo (see also Figures 4A and 4B for comparison).

(C–F) Transverse cryostat sections in the thoracic region of *Myf-5*$^{a2+/-}$ (C and D) and *Myf-5*$^{a2-/-}$ (E and F) E11 (42 somite) embryos reacted with both anti-β-gal (red, C and E) and anti-MyoD (green, D and F) antibodies. As a control for the anti-MyoD antibody, the mandibular arch appearing on the same section(F) is MyoD$^+$ (data not shown). β-gal$^+$ and MyoD$^+$ cells are clearly detectable in the myotome of the heterozygote (C and D). More sensitive X-Gal labeling reveals some β-gal$^+$ cells present ventrally (data not shown). In contrast, β-gal$^+$ cells in the homozygote are blocked dorsally and ventrally (E) and lack MyoD expression (double arrowheads in [F] indicate two MyoD$^+$ cells). Arrows (D) indicate the ventral somitic bud and the dorsal medial lip of the dermomyotome. dmy, dorsal myotome; vmy, ventral myotome; nt, neural tube. Scale bar, 25 μm (C–F).

a delay in *MyoD* transcript (n = 5) and protein (n = 3) accumulation in *Myf-5* null mice, suggesting that initial *MyoD* activation is dependent on the prior activation of *Myf-5*. Furthermore, this observation reveals that Pax-3–dependent *MyoD* activation occurs later than that by Myf-5.

Unsegmented Paraxial Mesoderm from *Sp* Homozygous Embryos Yields Significantly Reduced Numbers of MyoD-Expressing Cells in Explant Cultures

We have shown above that the early activation of *MyoD* is dependent on the prior activation of *Myf-5*. To evalute whether later *MyoD* activation is dependent on *Pax-3*, it was necessary to examine *Sp* homozygous embryos in experimental conditions in which the myogenic contribution of *Myf-5* would be reduced or eliminated. This condition can be achieved by using explants of UPM, cultured in the absence of axial structures (neural tube and notochord) that normally induce *Myf-5* but in the presence of dorsal ectoderm, which leads to *MyoD* activation. After a short period in culture, activation of *MyoD* in Myf-5$^+$ cells is negligible (Cossu et al., 1996a). We therefore cultured UPM from E9.5 *Sp* homozygous embryos without axial structures but including dorsal ectoderm. The explants were assayed with an anti-MyoD antibody after 60 hr in culture. Control cultures consisted of UPM from *Sp* homozygous embryos in the presence of axial structures. Explant cultures of *Sp* heterozygous embryos with and without axial structures served as a standard for these experiments. As expected, control cultures showed substantial numbers of MyoD$^+$ cells (Figure 6). Notably, in *Sp* homozygous cultures, UPM yielded strikingly reduced numbers of MyoD$^+$ cells, and this continued to be the case in older cultures (data not shown). In cultures of UPM from *Myf-5*$^{a2-/-}$ embryos, as expected, the numbers of MyoD$^+$ cells were equivalent in the presence or absence of axial structures and were

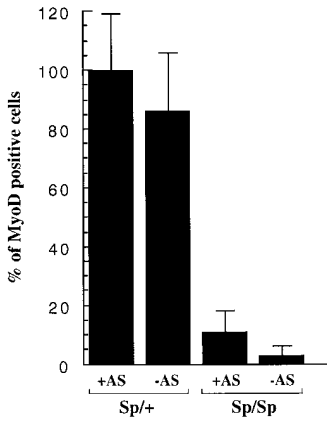

Figure 6. MyoD Expression Is Significantly Reduced in Explant Cultures of UPM from *Sp* Homozygous Embryos

UPM, including dorsal ectoderm, from E9.5 (18–24 somites) *Sp* heterozygous (*Sp*/+; n = 5) and *Sp* homozygous (*Sp*/*Sp*; n = 4) embryos was cultured for 60 hr with or without axial structures (AS; neural tube and notochord). Anti-MyoD antibody staining of cultures permitted MyoD$^+$ cells to be counted. Histograms are presented as a percentage of MyoD$^+$ cells in *Sp* heterozygous cultures with axial structures, which gave similar results to wild-type cultures (data not shown). Error bars, standard error of the mean.

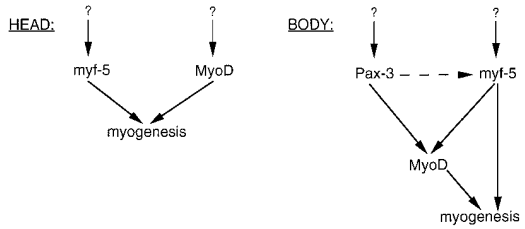

Figure 7. Model for the Genetic Hierarchies Operating in the Control of Skeletal Myogenesis

Arrows do not necessarily reflect a direct effect; dashed arrow represents a hypothetical interaction.

significantly higher than with *Sp* homozygous UPM (data not shown). This finding therefore confirms that *Pax-3* is required for the activation of the *MyoD* gene in conditions in which the *Myf-5* contribution is severely reduced. It is noteworthy that *MyoD* expression was also reduced in *Sp* homozygous embryos in the presence of axial structures. This suggests that *Pax-3* as well as *Myf-5* is involved in the activation of *MyoD* by the axial structures and is consistent with our in vivo observations.

Experiments in which the muscle differentiation marker MHC was detected with antibodies (data not shown) also clearly indicated that in the absence of axial structures, induction of myogenesis by dorsal ectoderm is severely impaired in *Sp* homozygous embryos. These findings therefore confirm that in conditions in which activation via *Myf-5* is severely reduced, a Pax-3–dependent *MyoD* activation pathway is uncovered.

Discussion

In this study, we used a loss-of-function approach in mice to evaluate the respective roles that the paired box transcription factor Pax-3 and the bHLH myogenic regulatory factors Myf-5 and MyoD play in programming skeletal myogenesis. We demonstrate that muscle progenitor cells in the body require the combined actions of Pax-3 and Myf-5 to make muscle, while Pax-3 does not appear to play a role in establishing nonsomitic head muscles. In the absence of these factors, *MyoD* is not activated and therefore cannot rescue myogenesis in the body, suggesting that *MyoD* acts genetically downstream of both *Pax-3* and *Myf-5* for the establishment of skeletal muscles in the body (Figure 7).

Muscle Progenitor Cell and Skeletal Muscle Perturbations in *Sp* Mice

By studying heterozygous mice in which the *nlacZ* reporter gene had been targeted into the *Myf-5* locus to facilitate the monitoring of muscle development, we confirm and extend previous observations on the *Sp* homozygous mouse. In addition to the absence of limb muscles, some shoulder, ventral body, and tongue muscles are missing (see also Franz et al., 1993; Bober et al., 1994; Goulding et al., 1994). We also show that the diaphragm, latissimus dorsi muscle, and muscles of the hypoglossal chord and ventral body wall are ablated in *Sp* homozygous embryos. All of these muscles are probably derived from the lateral part of the dermomyotome and by definition are of hypaxial origin. This raises the question of whether all hypaxial muscles are ablated in *Sp* mice, or whether *Pax-3* is required only for the formation of muscles that necessitate long-range migrations of precursor cells, as our results clearly suggest.

If we now consider perturbations in the somite itself in *Sp* mice, the most striking abnormality is the ablation of the somitic bud, which is derived from the lateral dermomyotome (see also Bober et al., 1994; Daston et al., 1996). The consequence of this perturbation on myotome formation is not clear. In the absence of a specific marker for laterally derived (hypaxial) myogenic cells, it is difficult to distinguish these cells from medially derived epaxial muscle that may have expanded laterally. Nevertheless, it is clear that *Sp* embryos show perturbations of myogenic progenitors and the myotome laterally. This observation is supported by our experiments with explants. In the absence of axial structures (neural tube and notochord), myogenesis by the medial route, which requires Myf-5, is blocked (Cossu et al., 1996b), and lateral myogenic induction by dorsal ectoderm can be analyzed. We provide evidence that under these conditions, UPM from *Sp* embryos was severely impaired in its ability to produce muscle. This was not the case when lateral-half somites from *Sp* embryos were transplanted into the limb bud (Daston et al., 1996); however, disruption of somite architecture has been reported to induce myogenesis (Gamel et al., 1995). In our experiments, we did not distinguish between migratory populations and those that will differentiate in the somite. Nevertheless, these observations suggest that lateral myogenesis by means of signals from the dorsal ectoderm is mediated mainly through *Pax-3* function.

A second important question is what happens to myogenic cells that are derived from the medial dermomyotome in the absence of Pax-3. *Pax-3* is expressed throughout the dermomyotome early, and subsequently these transcripts are concentrated in the lateral domain (Williams and Ordahl, 1994; Bober et al., 1994; Goulding et al., 1994). It is therefore very surprising that *MyoD* activation does not proceed in the *Sp/Myf-5*$^{a2-/-}$ double mutant, as it does in *Myf-5* null embryos. In fact, *Sp* embryos do show a subtle muscle phenotype in epaxial musculature derived from the medial dermomyotome (see also Franz et al., 1993). The *met* gene, which appears to be a direct downstream target of Pax-3 (Epstein et al., 1996; Yang et al., 1996), encodes a tyrosine kinase receptor that may also play a role in proliferation (Maina et al., 1996). Notably, *met*, which is expressed in the lateral dermomyotome, where it is necessary for the migration of cells to the limb (Bladt et al., 1995), is also expressed in the medial lip of the dermomyotome at the time when *Pax-3* is down-regulated in this region. Thus, at least one downstream gene in the *Pax-3* pathway is expressed in the medial part of the somite when myogenesis is taking place.

Pax-3 and *Myf-5* Act Genetically Upstream of *MyoD* and Together Are Essential for Myogenesis in the Body

Our analysis of *Sp/Myf-5*$^{a2-/-}$ double homozygous embryos demonstrates that skeletal muscles are absent in

the bodies of these animals. MHC and myogenin, markers of differentiated skeletal muscle, are not expressed, and furthermore the lack of desmin expression indicates that myoblasts are also absent. The trace amount of differentiated muscle cells that we detect may arise because of some leakiness of the *Sp* allele. Alternatively, it is possible that mammals have retained a vestige of a myogenic pathway that escapes the usual early dependence on the MyoD family of myogenic regulators (Smith et al., 1993). In Drosophila, a significant proportion of myogenic cells do not depend on the single *D-MyoD* (nautilus) gene (Bate, 1992).

In contrast to the body, nonsomitic head muscles are present in the double mutant; *MyoD* is activated and other muscle markers accumulate as expected, raising the possibility that *Pax-3* plays a key regulatory role in somitic mesoderm and not in more anterior paraxial and prechordal mesoderm, from which the majority of head muscles arise. A subset of tongue muscles are derived from the somites, and *Sp* homozygous mice have defects in tongue muscle development. In addition, we find that a group of neck muscles that extend from the head into the body are present in the double mutant. The mesodermal origin of the latter is not clear. A more detailed analysis of these and other head muscles should help to determine whether *Pax-3* function is indeed limited to somitic mesoderm. In support of this, we detect neither *Pax-3* nor *Pax-7* expression (see also Mansouri et al., 1996) in head muscles or their precursors.

MyoD Activation Is Dependent on Both Pax-3 and Myf-5

Previous analysis of the *Myf-5* null mutant showed that MyoD rescues muscle development (Braun et al., 1992). Based on that finding and the report that *MyoD* activation takes place normally in *Myf-5* null mice (Braun et al., 1994), it has been concluded that *MyoD* activation is independent of *Myf-5*. Therefore, given the phenotype of the *Sp/Myf-5*$^{a2-/-}$ double homozygous embryos, it might be expected that *MyoD* activation is Pax-3, not Myf-5, dependent. However, we show that in *Myf-5* null embryos, *MyoD* activation is delayed. The discrepancy between our results and those reported previously (Braun et al., 1994), at least with regard to cranial somites, may be explained by the presence of a group of shoulder muscles anterior to the forelimb that do not show the usual delay between *Myf-5* and *MyoD* activation; the development of these muscles is not perturbed in *Myf-5*$^{a2-/-}$ embryos. Our comparative analysis between control and *Myf-5*$^{a2-/-}$ embryos clearly demonstrates an initial dependence of *MyoD* activation on Myf-5 at most sites in the trunk of the embryo. It has been proposed, based on experiments with ES cells, that *MyoD* and *Myf-5* are activated in independent cell lineages and are not coexpressed (Braun and Arnold, 1996). Our observations on *Myf-5*$^{a2+/-}$ embryos and with explants show that *MyoD* is activated in medially derived muscle cells that have already activated *Myf-5* (Cossu et al., 1996a; Tajbakhsh et al., 1996a).

Unexpectedly, the delay in *MyoD* activation is also evident in the lateral aspect of the somite, where in explant experiments *MyoD* is preferentially activated (Cossu et al., 1996a). Preferential accumulation of MyoD in this domain has also been reported in vivo (Smith et al., 1994; Patapoutian et al., 1995; Cossu et al., 1996a). Our observations on the *Myf-5* null mutant, in which muscle progenitor cells are blocked in the lateral as well as the medial domain, also indicates that *Myf-5* is indeed activated laterally. Lateral activation of *Myf-5* may represent a subpopulation of myogenic precursors. In the absence of both Pax-3 and Myf-5, this lateral expression is ablated, suggesting that *Pax-3* is acting upstream of *Myf-5* in this region of the embryo.

How Do Pax-3 and Myf-5 Control Myogenesis?

In vitro experiments have shown that overexpression of *Myf-5* in a non–muscle cell results in *MyoD* activation (Weintraub et al., 1991). A simple explanation for the lack of MyoD in the *Sp/Myf-5*$^{a2-/-}$ double mutant is that *MyoD* is also transcriptionally activated by Pax-3. The explant experiments reported here suggest this. In keeping with this interpretation, in explant experiments with presomitic mesoderm, dorsal ectoderm activates *Pax-3* (Fan and Tessier-Lavigne, 1994) as well as *MyoD* (Cossu et al., 1996a). Furthermore, experiments with ectopically expressed *Pax-3* suggest that this may be the case (Maroto et al., 1997 [this issue of *Cell*]).

Other aspects of Pax-3 function have to be considered in this context. Pax-3 has been reported to inhibit myogenic differentiation under some conditions (Epstein et al., 1995), and this may be related to the fact that overexpression of *Pax* genes, either in vitro or as a result of a chromosomal rearrangement, transforms certain cell lines (Tremblay and Gruss, 1994). Since the *met* gene is expressed in the medial part of the dermomyotome after *Pax-3* has been down-regulated in this part of the somite (Yang et al., 1996), it is possible that Pax-3, perhaps through Met, is necessary for the amplification of a population of myogenic progenitor cells that subsequently express *MyoD*. Similarly, ablation of the lateral dermomyotome in *Sp* embryos, with loss of the somitic bud, may also point to the loss of a reservoir of Pax-3^{+} stem cells that would normally feed into the postmitotic myotome (Figure 5D).

Pax-3 is clearly involved in long-range cell migrations, probably by means of the Met receptor and its ligand, scatter factor (Bladt et al., 1995). It may also be critical for short-range migration within the somite. Again, the expression of the Met receptor in the medial as well as lateral domain of the dermomyotome and in body muscles that are probably of epaxial origin (Sonnenberg et al., 1993; Yang et al., 1996) is consistent with a role in short-range migration. In the head, muscle positioning as a result of growth rather than extensive cell migration may obviate the need for Pax-3, or alternatively, another gene functionally substitutes for *Pax-3* in the head.

From our analysis of the *Myf-5*$^{a2-/-}$ null embryos, we have demonstrated that in the absence of this myogenic factor, muscle progenitor cells migrate aberrantly and fail to localize to the cental aspect of the somite. We suggested that Myf-5 may "determine" the fate of myogenic progenitor cells by activating a cell surface component that permits them to respond correctly to positional cues in the embryo; in the absence of Myf-5, the

cells do not enter an environment that permits myogenesis to take place (Tajbakhsh et al., 1996b). Pax-3 may play a similar role. However, the inactivation of *Myf-5*, in contrast to that of *Pax-3*, does not appear to interfere with the elaboration of this muscle progenitor cell population or with their delamination from the dermomyotome (Tajbakhsh et al., 1996b). To evaluate the precise role that Pax-3 plays in myogenesis, it will be important to see whether *met*$^{-/-}$/*Myf-5*$^{a2-/-}$ double null mice have the same phenotype as *Sp*/*Myf-5*$^{a2-/-}$ double mutants. We have initiated experiments of this kind to investigate the respective roles of *Pax-3* and *Myf-5*, which, in the genetic hierarchy established in our study (Figure 7), act upstream of *MyoD* in the initiation of myogenesis.

Experimental Procedures

Generation of Embryos and Genotyping

Gene targeting of the *Myf-5* locus with the *nlacZ* (n, nuclear localization signal) reporter gene has been described previously (Tajbakhsh et al., 1996b). Heterozygous *Myf-5*$^{a2+/-}$ (129sv/C57BL6/DBA2) and *Sp* (C57BL6, Jackson Laboratories) mice were interbred to obtain double heterozygous animals. *Sp* /+/*Myf-5*$^{a2+/-}$ mice were then interbred to obtain *Sp*/*Myf-5*$^{a2-/-}$ double homozygous embryos. Mice carrying the *Myf-5*^{a2} mutation were also analyzed on an outbred (CD1) genetic background. To distinguish *Myf-5* mutant embryos in the litter, genotyping by polymerase chain reaction (PCR) of yolk sacs or a portion of the embryo was used to detect the wild-type (225 bp), heterozygous (225 and 414 bp), and homozygous (414 bp) alleles as described previously (Picard, 1994). A combination of three oligonucleotides was used: M5KO1, 5′-GGT GTC TCC TCT CTG CTG AAT CCA GGT AT (forward); M5KO2, 5′-AGG TGC ACG CAC GTG CTC CTC ACT GTC TGA (reverse); and M5KO3, 5′-CGC ATC GTA ACC GTG CAT CTG CCA GTT TGA (reverse). M5KO2 is located within the bHLH region that was deleted in the targeted allele, and M5KO3 is located in the *nlacZ* reporter gene. Alternatively, genotyping was carried out by Southern analysis or embryos were distinguished by their β-gal expression pattern, generally using rostral somites. The spontaneously arising *Sp* allele has a mutation in intron 3, resulting in the production of aberrantly spliced transcripts (Epstein et al., 1993) that can be detected by in situ hybridization. *Sp* embryos were identified by using specific primers spanning intron 3 and exon 4: *Sp4* (intron 3, forward), 5′-GAG AGG GTT GAG TAC GTT AGC-3′; *Sp2* (wild type, reverse), 5′-CGG CTG ATA GAA CTC ACT GGA-3′; and *Sp3* (mutant, reverse), 5′-CGG CTG ATA GAA CTC ACA CAC-3′. *Sp4* and *Sp2* (wild type) or *Sp4* and *Sp3* (*Sp*) were amplified (PCR product, 110 nucleotides) separately. *Sp* embryos were also readily identifiable by their spina bifida or exencephaly phenotype or both. Of 142 embryos analyzed between E10.5 and E14.5, 11 were *Sp*/*Myf-5*$^{a2-/-}$ double homozygous (frequency 7.7%; expected 6.25%). The double homozygous mutant phenotype was observed only when double heterozygous animals were interbred and not when *Sp*/+/*Myf-5*$^{a2+/-}$ mice were bred with *Sp* heterozygous or *Myf-5*$^{a2+/-}$ mice.

For genotyping, DNA was prepared (Laird et al., 1991), denatured (94°C for 15 min) in the presence of primers (100 ng each), and subjected to PCR in a 30 μl reaction for 35 cycles: 94°C for 45 s, 60°C for 1 min, and 72°C for 1 min using Taq (Cetus) polymerase and the manufacturer's buffer in the presence of 300 mM $MgCl_2$ and 0.3% Tween-20.

Detection of Transcripts on Whole-Mount Embryos and Embryo Sections

Embryos at different stages (plug date, E0.5) were fixed in fresh 4% paraformaldehyde and prepared for in situ hybridization with ^{35}S antisense probes for paraffin sections (Tajbakhsh and Houzelstein, 1995) or digoxygenin-11-UTP (Boehringer) probes for whole embryos (Henrique et al., 1995) with some modifications. For whole-mount in situ hybridizations, postantibody washes were for about 2 days, and the revealing reaction was carried out for a few hours to 2 days with changes of the solution (alkaline phosphatase substrate, Boehringer). In some cases, embryos were stained briefly with X-Gal (Tajbakhsh and Buckingham, 1994) prior to hybridization. Antisense probes used during this study were *MyoD* and *myogenin* (Sassoon et al., 1989), *Pax-3* (519 bp PstI/HindIII fragment from the 3′ end of cDNA), and *Pax-7* (Jostes et al., 1990; kindly provided by P. Gruss). Slides were processed for autoradiography, developed after 8–10 days, and photographed with a Zeiss Axiophot microscope. Photographs of whole-mount stained embryos were taken with an Olympus SZH10 stereomicroscope.

Explant Cultures and Immunofluorescence

E9.5 embryos were dissected at room temperature in RPMI (GIBCO–BRL) medium, and the UPM with dorsal ectoderm but without most of the lateral mesoderm was removed from wild-type, heterozygous, and homozygous embryos. At this stage, the UPM would give rise to somites of the interlimb region. The remainder of the embryo was used for genotyping. Axial structures were dissected away from somites using 0.1% pancreatin and 0.1% trypsin for 2 min at 4°C, and the reaction was stopped with the addition of medium containing serum. Individual explants were grown on a feeder layer of 10T1/2 cells in RPMI supplemented with 10% decomplemented (56°C, 30 min) fetal calf serum. Immunofluorescence was carried out (Tajbakhsh and Buckingham, 1995; Cossu et al., 1996a) with the following: a polyclonal anti-MyoD (a gift from J. Harris), monoclonal anti-MHC MF20 antibody, anti-MHC (polyclonal), and anti-β-gal (monoclonal, Sigma). Secondary antibodies were conjugated with Texas-Red (Amersham; Figure 3), rhodamine (Sigma; Figure 5), or peroxidase (Sigma). MyoD$^+$ cells were scored per explant experiment after 60 hr. Cell survival, as evaluated by Hoechst 33258 staining, appeared similar in *Sp* heterozygous and homozygous embryo cultures.

Acknowledgments

This work was supported by grants from the Pasteur Institute, the Centre National de la Recherche Scientifique, the Association Française contre les Myopathies, Italian Telethon A.67, and the Ministère de l'Education Nationale, de l'Enseignement Supérieur et de la Recherche. We thank P. Gruss and J. Harris for kindly providing *Pax-3* and *Pax-7* probes and MyoD antibody, respectively, and K. Vogan for providing the *Pax-3* intron sequence. We are grateful to P. Tremblay, R. Sporle, and members of the Buckingham laboratory for helpful discussions; R. Kelly for critical reading of the manuscript; and M. Polimeni for her scientific contribution.

Received December 16, 1996; revised February 11, 1997.

References

Bate, M. (1992). Mechanisms of muscle patterning in Drosophila. Semin. Dev. Biol. *3*, 267–275.

Bladt, F., Riethmacher, D., Isenmann, S., Aguzzi, A., and Birchmeier, C. (1995). Essential role for the c-met receptor in the migration of myogenic precursor cells into the limb bud. Nature *376*, 768–771.

Bober, E., Franz, T., Arnold, H.H., Gruss, P., and Tremblay, P. (1994). Pax-3 is required for the development of limb muscles: a possible role for the migration of dermomyotomal muscle progenitor cells. Development *120*, 603–612.

Braun, T., and Arnold, H.-H. (1996). *myf-5* and *myoD* genes are activated in distinct mesenchymal stem cells and determine different skeletal muscle cell lineages. EMBO J. *15*, 310–318.

Braun, T., Bober, E., Rudnicki, M.A., Jaenisch, R., and Arnold, H.H. (1994). MyoD expression marks the onset of skeletal myogenesis in Myf-5 mutant mice. Development *120*, 3083–3092.

Braun, T., Rudnicki, M.A., Arnold, H.-H., and Jaenisch, R. (1992). Targeted inactivation of the muscle regulatory gene *Myf-5* results in abnormal rib development and perinatal death. Cell *71*, 369–382.

Buckingham, M. (1992). Making muscle in mammals. Trends Genet. *8*, 144–149.

Christ, B., and Ordahl, C.P. (1995). Early stages of chick somite development. Anat. Embryol. *191*, 381–396.

Cossu, G., Kelly, R., Tajbakhsh, S., Di Donna, S., Vivarelli, E., and Buckingham, M. (1996a). Activation of different myogenic pathways: myf-5 is induced by the neural tube and MyoD by the dorsal ectoderm in mouse paraxial mesoderm. Development *122*, 429–437.

Cossu, G., Tajbakhsh, S., and Buckingham, M. (1996b). How is myogenesis initiated in the embryo? Trends Genet. *12*, 218–223.

Daston, G., Lamar, E., Olivier, M., and Goulding, M. (1996). Pax-3 is necessary for migration but not differentiation of limb muscle precursors in the mouse. Development *122*, 1017–1027.

Epstein, D.J., Vogan, K.J., Trasler, D.G., and Gros, P. (1993). A mutation within intron 3 of the Pax-3 gene produces aberrantly spliced mRNA transcripts in the splotch (Sp) mouse mutant. Proc. Natl. Acad. Sci. USA *90*, 532–536.

Epstein, J.A., Lam, P., Jepeal, L., Maas, R.L., and Shapiro, D.N. (1995). Pax3 inhibits myogenic differentiation of cultured myoblast cells. J. Biol. Chem. *270*, 11719–11722.

Epstein, J.A., Shapiro, D.N., Cheng, J., Lam, P.Y., and Maas, R.L. (1996). Pax3 modulates expression of the c-Met receptor during limb muscle development. Proc. Natl. Acad. Sci. USA *93*, 4213–4218.

Fan, C.M., and Tessier-Lavigne, M. (1994). Patterning of mammalian somites by surface ectoderm and notochord: evidence for sclerotome induction by a hedgehog homolog. Cell *79*, 1175–1186.

Franz, T., Kothary, R., Surani, M.A., Halata, Z., and Grim, M. (1993). The Splotch mutation interferes with muscle development in the limbs. Anat. Embryol. *187*, 153–160.

Gamel, A.J., Brand-Saberi, B., and Christ, B. (1995). Halves of epithelial somites and segmental plate show distinct muscle differentiation behavior in vitro compared to entire somites and segmental plate. Dev. Biol. *172*, 625–639.

Goulding, M., Lumsden, A., and Paquette, A.J. (1994). Regulation of Pax-3 expression in the dermomyotome and its role in muscle development. Development *120*, 957–971.

Hasty, P., Bradley, A., Morris, J.H., Edmondsnon, D.G., Venuti, J.M., Olson, E.N., and Klein, W.H. (1993). Muscle deficiency and neonatal death in mice with a targeted mutation in the *myogenin* gene. Nature *364*, 501–506.

Henrique, D., Adam, J., Myat, A., Chitnis, A., Lewis, J., and Ish-Horowicz, D. (1995). Expression of a Delta homologue in prospective neurons in the chick [see comments]. Nature *375*, 787–790.

Jostes, B., Walther, C., and Gruss, P. (1990). The murine paired box gene, Pax7, is expressed specifically during the development of the nervous and muscular system. Mech. Devel. *33*, 27–37.

Kenny-Mobbs, T., and Thorogood, P. (1987). Autonomy of differentiation in avian branchial somites and the influence of adjacent tissues. Development *100*, 449–462.

Laird, P.W., Zijderveld, A., Linders, K., Rudnicki, M.A., Jaenisch, R., and Berns, A. (1991). Simplified mammalian DNA isolation procedure. Nucleic Acids Res. *19*, 4293.

Maina, F., Casagranda, F., Audero, E., Simeone, A., Comoglio, P.M., Klein, R., and Ponzetto, C. (1996). Uncoupling of Grb2 from the Met receptor in vivo reveals complex roles in muscle development. Cell *87*, 531–542.

Mansouri, A., Stoykova, A., Torres, M., and Gruss, P. (1996). Dysgenesis of cephalic neural crest derivatives in Pax7−/− mutant mice. Development *122*, 831–838.

Marcelle, C., Wolf., J., and Bronner-Fraser, M. (1995). The *in vivo* expression of the FGF receptor FREK mRNA in avian myoblasts suggests a role in muscle growth and differentiation. Dev. Biol. *172*, 100–114.

Maroto, M., Reshef, R., Münsterberg, A.E., Koester, S., Goulding, M., and Lassar, A.B. (1997). Ectopic Pax-3 activates MyoD and Myf-5 expression in embryonic mesoderm and neural tissue. Cell *88*, this issue.

Nabeshima, Y., Hanaoka, K., Hayasaka, M., Esumi, E., Li, S., Nonaka, I., and Nabeshima, Y. (1993). Myogenin gene disruption results in perinatal lethality because of severe muscle defect. Nature *364*, 532–535.

Olson, E.N., Arnold, H.-H., Rigby, P.W. J., and Wold, B.J. (1996). Know your neighbors: three phenotypes in null mutants of the myogenic bHLH gene *MRF4*. Cell *85*, 1–4.

Ott, M.-O., Bober, E., Lyons, G., Arnold, H., and Buckingham, M. (1991). Early expression of the myogenic regulatory gene, *myf-5*, in precursor cells of skeletal muscle in the mouse embryo. Development *111*, 1097–1107.

Patapoutian, A., Yoon, J.K., Miner, J.H., Wang, S., Stark, K., and Wold, B. (1995). Disruption of the mouse MRF4 gene identifies multiple waves of myogenesis in the myotome. Development *121*, 3347–3358.

Picard, J.K. (1994). A PCR strategy to distinguish heterozygous and homozygous gene "knockout" transgenic mice. Transgenics *1*, 241–243.

Pourquié, O., Fan, C.-M., Coltey, M., Hirsinger, E., Wanatabe, Y., Bréant, C., Francis-West, P., Brickell, P., Tessier-Lavigne, M., and Le Douarin, N.M. (1996). Lateral and axial signals involved in avian somite patterning: a role for BMP4. Cell *84*, 461–471.

Rudnicki, M.A., Braun, T., Hinuma, S., and Jaenisch, R. (1992). Inactivation of *MyoD* in mice leads to up-regulation of the myogenic HLH gene *Myf-5* and results in apparently normal muscle development. Cell *71*, 383–390.

Rudnicki, M.A., Schneglesberg, P.N.J., Stead, R.H., Braun, T., Arnold, H.-H., and Jaenisch, R. (1993). MyoD or Myf-5 is required for the formation of skeletal muscle. Cell *75*, 1351–1359.

Sassoon, D., Lyons, G.E., Wright, W., Lin, V., Lassar, A., and Weintraub, H. (1989). Expression of two myogenic regulatory factors: myogenin and MyoD1 during mouse embryogenesis. Nature *341*, 303–307.

Smith, T.H., Block, N.E., Rhodes, S.J., Konieczny, S.F., and Miller, J. B. (1993). A unique pattern of expression of the four muscle regulatory factor proteins distinguishes somitic from embryonic, fetal and newborn mouse myogenic cells. Development *117*, 1125–1133.

Smith, T.H., Kachinsky, A.M., and Miller, J.B. (1994). Somite subdomains, muscle cell origins, and the four muscle regulatory factor proteins. J. Cell Biol. *127*, 95–105.

Sonnenberg, E., Meyer, D., Weidner, K.M., and Birchmeier, C. (1993). Scatter factor/hepatocyte growth factor and its receptor, the c-met tyrosine kinase, can mediate a signal exchange between mesenchyme and epithelia during mouse development. J. Cell Biol. *123*, 223–235.

Strachan, T., and Read, A.P. (1994). PAX genes. Curr. Opin. Genet. Dev. *4*, 427–438.

Tajbakhsh, S., and Buckingham, M.E. (1994). Mouse limb muscle is determined in the absence of the earliest myogenic factor myf-5. Proc. Natl. Acad. Sci. USA *91*, 747–751.

Tajbakhsh, S., and Buckingham, M.E. (1995). Lineage restriction of the myogenic conversion factor myf-5 in the brain. Development *121*, 4077–4083.

Tajbakhsh, S., and Houzelstein, D. (1995). In situ hybridization and β-galactosidase: a powerful combination for analysing transgenic mice. Trends Genet. *11*, 42.

Tajbakhsh, S., Bober, E., Babinet, C., Pournin, S., Arnold, H., and Buckingham, M. (1996a). Gene targeting the myf-5 locus with nlacZ reveals expression of this myogenic factor in mature skeletal muscle fibres as well as early embryonic muscle. Dev. Dyn. *206*, 291–300.

Tajbakhsh, S., Rocancourt, D., and Buckingham, M. (1996b). Muscle progenitor cells failing to respond to positional cues adopt non-myogenic fates in *myf-5* null mice. Nature *384*, 266–270.

Tremblay, P., and Gruss, P. (1994). Pax: genes for mice and men. Pharmacol. Ther. *61*, 205–226.

Wachtler, F., and Christ, B. (1992). The basic embryology of skeletal muscle formation in vertebrates: the avian model. Semin. Dev. Biol. *3*, 217–227.

Weintraub, H., Davis, R., Tapscott, S., Thayer, M., Krause, M., Benezra, R., Blackwell, T.K., Turner, D., Rupp, R., Hollenberg, S., et al. (1991). The MyoD gene family: nodal point during specification of the muscle cell lineage. Science *251*, 761–766.

Williams, B.A., and Ordahl, C.P. (1994). Pax-3 expression in segmental mesoderm marks early stages in myogenic cell specification. Development *120*, 785–796.

Yang, X.M., Vogan, K., Gros, P., and Park, M. (1996). Expression of the met receptor tyrosine kinase in muscle progenitor cells in somites and limbs is absent in Splotch mice. Development *122*, 2163–2171.